Elsevier Editorial System(tm) for Medical Engineering & Physics
Manuscript Draft

Manuscript Number:

Title: Subject-specific musculoskeletal parameters of wrist flexors and extensors estimated by an EMG-driven musculoskeletal model

Article Type: Paper

Section/Category: Regular Issue Paper

Keywords: Wrist; EMG; neuromusculoskeletal model; flexors; extensors; estimation

Corresponding Author: Dr Francesco Maria Colacino, Ph.D.

Corresponding Author's Institution: University of Southampton

First Author: Francesco Maria Colacino, Ph.D.

Order of Authors: Francesco Maria Colacino, Ph.D.; Emiliano Rustighi, Ph.D.; Brian R Mace, Ph.D.

Abstract: An EMG-driven musculoskeletal model is implemented to estimate subject-specific musculoskeletal parameters such as the optimal physiological muscle length, the tendon slack length and the maximum isometric muscle force of flexor and extensor muscle groups crossing the wrist, as well as biomechanical indexes to quantify the muscle operating range, the stiffness of the musculotendon actuators, and the contribution of the muscle fibers to the joint moment.
Twelve healthy subjects (11 males and 1 female, mean age 31.1 ± 8.7 years) were instructed to perform isometric maximum voluntary contractions of wrist flexors and extensors. Recorded EMGs were used as input to the model and the root mean square error (RMSE) between measured and predicted torque was minimised to estimate the subject-specific musculotendon parameters. The model was validated and the RMSE and the normalised RMSE calculated during estimation and validation phases are compared.
Estimated subject-specific musculoskeletal parameters vary in a physiological range, while the biomechanical indexes are in agreement with previously published data.
The proposed methodology proved to be effective for the in-vivo estimation of physiological parameters of the musculotendon complex and has potential as an investigative tool to distinguish aetiological differences among subjects affected by musculoskeletal disorders.

Introduction

Modelling the neuronal and mechanical elements underlying human movements can give helpful insight for the design of physiologically fine-tuned rehabilitation protocols for people affected by spinal cord injury, stroke, head injuries, as well as cerebral palsy and multiple sclerosis [1-2]. Neuromusculoskeletal modelling could be exploited as an investigative tool to discriminate between biomechanical and neural causes of musculoskeletal disorders or diseases affecting the nervous system. Indeed, pathological conditions could be inferred by analyzing deviations of specific indexes from normal values. This would provide additional insights into the dynamic interactions among the elements involved in the execution of motor tasks that would be difficult or even impossible to obtain from physiological studies alone [3]. Musculoskeletal models developed so far can be mainly categorized as inverse dynamic models and forward dynamic models [4-6]. There is yet another approach which merges the above two and can be used to calibrate and validate a musculoskeletal model: a hybrid forward and inverse dynamic model [4, 7].

In this paper, by using a hybrid approach, an EMG-driven musculoskeletal model of a one degree of freedom wrist joint was implemented and validated with the aim of estimating the biomechanical parameters of wrist flexors and extensors. EMGs and torques exerted in flexion/extension, recorded in healthy subjects during maximum voluntary contractions (MVCs) of selected wrist flexors and extensors, were used as input to the model in order to estimate in-vivo subject-dependent musculotendon parameters. The model was finally validated and values of indexes characterizing the biomechanics of contractions calculated.

In the next section the model of the musculotendon unit and the equations used to mimic the anatomy of the wrist joint will be described together with the experiments performed and the procedure for parameter estimation. The equations adopted from other works are detailed herein together with those specifically related to the present work. Following that the values

of the estimated parameters and the validation of the model will be described in the results section. Finally our findings are discussed and compared with data in the literature.

Materials and methods

Model Description

The instantaneous total force, F_{MT}, exerted by a musculotendon unit was calculated by means of a lumped Hill-type musculotendon model [8] as

$$F_{MT}(\theta,t) = F_M = F_T = \left[\widetilde{FL}_a \cdot \widetilde{FV} \cdot a + \widetilde{FL}_p\right] \cdot F_{oM} \qquad (1)$$

where t is time, θ is the angular position of the wrist, $F_M(\theta,t)$ is the muscle force, $F_T(\theta,t)$ is the tendon unit force, $\widetilde{FL}_a(\theta,t)$ and $\widetilde{FL}_p\ (\theta,t)$ are respectively the normalised active and passive muscle force-length relationships, $\widetilde{FV}(\theta,t)$ is the normalised muscle force-velocity relationship, F_{oM} is the maximum isometric muscle force and *a(t)* is the activation level (Fig. 1). This was estimated from linear envelope processing of measured raw EMG signals as described below. Muscle and tendon were considered to be connected in series, while the pennation angle was disregarded for this joint [9]. Normalisations were applied according to the scaling approach adopted in [8]. Parameter values are listed in Table I.

The EMG signal was related to muscle activation *a(t)* as in Buchanan et al. [5]. A normalised, rectified, filtered EMG*, nrfEMG (t)*, was first transformed to the neural excitation *u(t)* by means of a first-order differential equation, that is

$$\frac{du(t)}{dt} + \left[\frac{1}{\tau_{act}} \cdot \left(\beta + (1-\beta) \cdot nrfEMG(t)\right)\right] \cdot u(t) = \frac{1}{\tau_{act}} \cdot nrfEMG(t), \qquad (2)$$

where the constant $\beta\,(0 < \beta < 1)$ was set as in Zajac [8] equal to $\beta = \tau\_act/\tau_{deac}$ with τ_{act} and τ_{deact} time constants defining the build-up in activation for excited or relaxed muscle. In particular, a relaxed muscle (*u(t)* = 0) activates more slowly than an excited one (*u(t)* = 1),

that is $\tau_{act} < \tau_{deact}$. Then, *u(t)* was related to the muscle activation *a(t)* according to the following non-linear relationship

$$a(t) = \frac{e^{Au(t)} - 1}{e^{A} - 1} \tag{3}$$

where the constant *A* must be determined during the calibration process.

The active muscle force-length relationship $\widetilde{FL_a}(\theta, t)$ was described as a normalised activation-dependent quadratic function of the normalised muscle length [5, 10], that is:

$$\widetilde{FL_a}(\theta, t) = k \cdot \widetilde{L_M}(\theta, t)^2 - 2 \cdot k \cdot \widetilde{L_M}(\theta, t) + k + 1. \tag{4}$$

It represents a parabolic curve normalised with respect to the maximum isometric muscle fibre force, F_{oM}, and function of the normalised muscle length $\widetilde{L_M}(\theta, t)$ (i.e. $\widetilde{L_M}(\theta, t) = \frac{L_M(\theta,t)}{L_{oM}}$), with $L_{oM}(t)$ the optimal physiological muscle length. The maximum isometric muscle force, F_{oM}, is the force developed by a muscle when it is maximally stimulated at its optimal physiological length, $L_{oM}(t)$. In turn, $L_{oM}(t)$ varies with the level of activation *a(t)* according to the relationship [5]

$$L_{oM}(t) = L_{oM}\{\lambda[1 - a(t)] + 1\}. \tag{5}$$

The term λ defines the amount of optimal fibre length increase as the activation decreases. The factor *k* is related to a scaling factor *d* as $k = -1/d^2$.

The normalised passive muscle force-length relationship, $\widetilde{FL_p}(\theta, t)$ was described as [5]

$$\widetilde{FL_p}(\theta, t) = \frac{e^{10(\widetilde{L_M}(\theta,t)-1)}}{e^{5}} \tag{6}$$

where $\widetilde{FL_p}(\theta, t)$ is normalised with respect to F_{oM} and $\widetilde{L_M}(\theta, t)$ is the muscle length normalised with respect to $L_{oM}(t)$.

The force-velocity relationship $\widetilde{FV}(\theta, t)$ normalised with respect to F_{oM} was described by the relationship [10]

$$\widetilde{FV}(\theta,t) = \frac{aa}{1 + e^{[bb(\widetilde{V_M}(\theta,t) - cc)]}} \tag{7}$$

where, *aa*, *bb*, and *cc* are appropriate constants and $\widetilde{V_M}(\theta,t)$ is the muscle velocity normalised with respect to the maximal contraction velocity $V_{max}(t) = 10 \cdot L_{oM}(t)$ [8]. By this formula, both eccentric (i.e. lengthening) and concentric (i.e. shortening) contractions are taken into account.

The normalised tendon force, $\tilde{F}_{K_T}(\theta,t)$, was modeled as in [5]

$$\begin{cases} \tilde{F}_{K_T} = 0 & \varepsilon \le 0 \\ \tilde{F}_{K_T} = 1480.3 \cdot \varepsilon^2 & 0 < \varepsilon < 0.0127 \\ \tilde{F}_{K_T} = 37.5 \cdot \varepsilon - 0.2375 & \varepsilon \ge 0.0127 \end{cases} \tag{8}$$

where $\tilde{F}_{K_T}(\theta,t)$ was normalised with respect to F_{oM}. The tendon strain was defined as $\varepsilon(\theta,t) = (L_T(\theta,t) - L_{TS})/L_{TS}$, where $L_T(\theta,t)$ is the tendon length and L_{TS} is the tendon slack length, i.e. the length beyond which a tendon starts carrying load (i.e. $\varepsilon > 0$).

The wrist angle was defined as zero with the hand in neutral position and positive (negative) as the wrist was flexed (extended). The instantaneous muscle length, $L_M(\theta,t)$, was given by [10-11]

$$L_M(\theta,t) = L_{MT}(\theta) - L_T(\theta,t) = L_{TS} + 1.2 \cdot L_{oM} + \Delta L_{MT}(\theta) - L_T(\theta,t) \tag{9}$$

For numerical stability, the muscle mass, M_m [12-13] was added to the model and the tendon unit comprised a damper $C(\theta,t)$ connected in parallel to the spring $K_T(\theta,t)$ (Fig. 1). The musculotendon dynamics was thus governed by

$$F_M(\theta,t) = M_m \cdot \ddot{L}_T(\theta,t) + C(\theta,t) \cdot \dot{L}_T(\theta,t) + F_{K_T}(\theta,t), \tag{10}$$

where $F_{K_T}(\theta,t)$ is the tendon force contribution due to the spring of the tendon unit and $C(\theta,t)$ is the viscous coefficient of the dashpot taken to be equal to

$$C(\theta,t) = \sqrt{4 \cdot M_m \cdot \left(F_{K_T}(\theta,t)/L_T(\theta,t)\right)}. \tag{11}$$

Equation (11) ensured a physiological critically-damped second order behavior [14-15].

Experiments

The experimental protocol was approved by the Human Experimentation Safety Committee of the University of Southampton and informed consent was obtained from each subject.

An instrumented armchair allowed seven pre-calibrated hand positions with the wrist angle in the range of +30° (flexion) to -30° (extension) with 10° intervals (Fig. 2). A CE approved Data Logger from MIE Medical Research Ltd. was used as a data acquisition system. The exerted torques were measured by a calibrated strain gauge load cell. All of the signals were sampled synchronously at 1000 Hz. A reference for aligning the wrist rotation axis was used. Twelve healthy subjects (mean age 31.1 ± 8.7 years) were instructed to perform three isometric flexion/extension MVCs at each position for 5 s, with 10 s rest between subsequent contractions. In total, 14 measurements were recorded for each subject. As Fig. 2 shows, the hand was in neutral orientation, while the forearm, arm (vertical), and elbow (flexed at 90°), were constrained. The shoulder was comfortably positioned. For the flexors, surface EMG electrodes were properly positioned equidistant from the motor point of Flexor Carpi Ulnaris (FCU), Flexor Carpi Radialis (FCR) and Flexor Digitorum Superficialis (FDS). For the extensors, EMG electrodes were positioned close to the motor point of extensor carpi radialis longus (ECRL). Thus, one EMG signal for flexion and one for extension were simultaneously recorded.

In what follows, the word ‘flexors’ means FCU, FCR and FDS lumped together, unless otherwise stated, while the word ‘extensors’ is used as a synonym of ECRL.

Parameter Estimation

The musculoskeletal parameters to be estimated were: the optimal physiological muscle length, L_{oM}; the maximum isometric muscle force, F_{oM}; the tendon slack length, L_{TS}; the

coefficient A; the moment arm, $MA(\theta)$; the musculotendon length change, $\Delta L_{MT}(\theta)$. The latter two parameters were allowed a 10% variation with respect to values obtained from [11] in order to take into account possible inaccuracies in the determination of the wrist angle. The coefficient A was constrained between -3 and 0 [5]. The remaining parameters were constrained to vary in physiologically meaningful ranges. In particular, F_{oM} and L_{TS} were constrained between 20 and 2000 N and 10 and 40 cm, respectively. For L_{oM} the lower bound was equal to 1 cm for both flexors and extensors, while the upper bound was equal to 10 cm for the flexors and no upper bound was set for the extensors.

Having constructed the model, the EMGs were used as input, while the predicted joint moments were compared to the measured moments exerted by the hand. The calculated root mean square error (RMSE) between the predicted and measured joint moments was used as the objective function to be minimized for the estimation of the six parameters. The optimization algorithm employed a gradient descent approach based on a Hessian (i.e. the second derivatives of the Lagrangian) and was implemented by using the Matlab function *fmincon*, which finds the minimum of constrained nonlinear multivariable function. Values in [16] were used as initial estimates of the corresponding parameters during the optimization process. The normalised RMSE (NRMSE) was also calculated as the ratio of RMSE to the maximum value of the measured torque in the same trial.

The great majority of the EMG measurements showed high firing level at rest (up to half of its range) when no contraction occurred. In order not to obtain a biased estimate, the parameters were estimated by exclusively using data corresponding to the contraction phases, while some values of the envelope EMG were used as a threshold to distinguish rest from contraction phases: EMG values above the threshold implied muscle contraction. The threshold was set according to a selected value of the gradient with respect to time of the envelope EMG (which varies between 0 and 1). In particular, a difference of 0.2 between two

EMG values separated by 400 samples on the ascending part of the data was used to identify the instants at which a contraction could be considered as begun, while a difference of 0.04 between two EMG values separated by 400 samples on the descending part of the same data was used to identify the instants at which a contraction could be considered as terminated.

It should be noted that 6 out of 7 measurements recorded for each subject and each muscle group were used for the estimation process. Measurements at 0° were only used during the validation process

It should be noted that the validation of the estimated parameters was carried out with measurements at 0°, while the measurements recorded for each subject and each muscle group at the remaining six positions were used for the estimation process. Co-contractions were disregarded whenever recorded.

It should be noted that the validation of the estimated parameters at 0° is shown hereafter, while a leave-one-out cross-validation (LOOCV) was carried out to assess how the estimation results can generalise to an independent input data set. Regarding the LOOCV, for each subject, the parameters in a prescribed position, calculated by averaging the estimated values in correspondence of the remaining six wrist angles, were used as input to the model to compute the torque. The procedure was repeated alternatively for each position and the RMSE and NRMSE values were calculated every time.

Finally, a sensitivity index (SI) was calculated to assess the influence of the estimated parameters on RMSE. The SI was calculated as in Eq. (12):

$$SI = \left| \frac{\frac{\Delta RMSE}{RMSE}}{\frac{\Delta P}{P}} \right|. \tag{12}$$

For each subject, each parameter was varied by ±5% (ΔP) with respect to the estimated value (P) and the RMSE variation ($\Delta RMSE$) computed.

Co-contractions were disregarded whenever recorded.

Results

Estimated Parameters

Data from three subjects for flexors and two subjects for extensors were neglected since they did not show any significant variation of the EMG signal between phases at rest and during contraction.

Table II compares estimated values of L_{oM}, F_{oM}, and L_{TS} (average ± standard deviation (SD) over six positions in the range [-30°,...,+30°] without measurements at 0° for all of the subjects) with values of the corresponding parameters as listed in [9, 16]. Ranges for the same values are also listed in Table II. Note that Garner and Pandy [9] and Holzbaur et al. [16] refer to, review and report a wide range of values. The average values of *MA* are shown later in Fig. 5, while the values of the two remaining parameters ΔL_{MT}, and A are not listed here for the sake of brevity.

With regard to the outcome of the SI analysis, it was found that changes in RMSE were the highest for changes in F_{oM} and *MA*, i.e. SI values were the highest for these two parameters and equal respectively to 2.58 (±1.39) and 2.47 (±1.56). The SI values of the remaining parameters L_{oM}, ΔL_{MT}, A and L_{TS} were equal to 0.28 (±0.24), 0.17 (±0.17), 0.09 (±0.15) and 0.08 (±0.05), respectively.

Model Validation

During validation both the estimated parameters and the EMGs recorded with the hand at 0° were used as input to the model. The predicted joint moments were compared to those measured at the same position. Fig. 3 shows one example which was selected since its RMSE and NRMSE values were representative of the average of the same quantities (Table II). When calculating the error, the predicted torque was assumed to equal the measured torque

when at rest, so that only model errors during the contraction phase contribute to the RMSE. This ensured consistency of the RMSE and NRMSE calculation during both estimation and validation. The average (±SD) RMSE and NRSME values calculated over all of the subjects during estimation (over six positions in the range [-30°,...,+30°]) and validation (at 0°) are listed in Table II. The same table contains the results for LOOCV.

Fig. 4 shows a comparison between predicted and measured maximum moments averaged over all of the subjects together with values from [9, 17-18]. The highest individual measured (M_{meas}) and predicted, (M_{pred}) moments as well as the highest overall measured (M^{TOT}_{meas}) and predicted (M^{TOT}_{pred}) moments for both flexors and extensors are listed in Table II. It should be noted that during flexor experiments the majority of the highest peaks occurred mainly when the wrist was in extension, while during extensor experiments they mainly occurred when the wrist was in flexion.

In Fig. 5 average values of *MA* together with average estimated forces at each position for both flexors and extensors are shown. The *MA* curves refer to the average *MA* values estimated at each position for all of the subjects. In the same figure, the curves labelled Estimated Force I and II were respectively calculated as the ratio of the average moments of the predicted and measured torques to the average estimated *MA* values. The highest average values of the estimated forces, $F_{EST\ I}$ and $F_{EST\ II}$, are listed in Table II. As for the moments, the wrist positions with the highest peaks were mainly found in extension during flexor experiments and in flexion during extensor experiments.

Fig. 6 shows the mean operating range of flexors and extensors on the isometric normalised force-length curve. The two diamond markers on the figure enclose the average operating range of wrist flexors, while the two triangle markers define the operating range of wrist extensors. Both the ranges were calculated by averaging the extreme values computed for each subject in the whole range of motion (±30°). The operating ranges of FCU, FCR and

ECRL muscles as reported in Loren et al. [19] and Gonzalez et al. [18] were adapted and are shown on the same figure for comparison.

Two indexes were also calculated [7] (Table II). The first index is the ratio of the tendon slack length to the optimal muscle length, L_{TS}/L_{oM}. This index relates to the stiffness of the wrist flexion/extension musculotendon actuators being smaller for stiffer actuators [8]. The second index is the ratio of the optimal muscle length to the average moment arm, L_{oM}/MA_{ave}: if its value increases, both the muscle excursion and the muscle contribution to the joint moment decrease, while the influence of *MA* increases [20].

Discussion

This one degree of freedom model of the wrist joint involves simplifications. First, it is based on the assumption that flexors act as a lumped muscle group and no distinction is made between the various flexors involved in wrist flexion. Regarding the extensors, only the ECRL contribution is taken into account and extension is ascribed to this latter muscle only. This certainly biases the results which could be improved by acquiring more EMGs, thus allowing contributions from other muscles during MVCs to be discriminated. Fig. 3A is representative of such a situation: even though the magnitude of the envelope EMG is similar for each contraction, the measured torque of the first contraction is larger than the torque for the other two and the predicted torque does not predict it well. Furthermore, the level of co-contraction of the antagonists could be taken into account as well. Secondly, no bone surface geometry, joint kinematics or muscle path geometry is considered. To overcome this limitation, scaled three-dimensional models provided by commercially available software such as SIMM (MusculoGraphics Inc., Chicago, USA) or AnyBody (AnyBody Technology, Aalborg, Denmark) could be used. Additionally, a newer approach worth mentioning is an image-based musculoskeletal modeling technique to obtain a detailed description of

musculoskeletal dynamics, complex muscle architecture, joint kinematics and muscle *MA*s as well as muscle tissue deformation in presence of disease [21]. Having said this, the simple model still predicts the output torques reasonably well and the choice of a more complex model should be considered carefully bearing in mind the number and accuracy of measured input variables that might be available. Lastly, the model was validated using healthy subjects only. Future work will include the use of the model with data gathered from patients affected by sensory-motor interaction diseases (e.g. stroke patients) so that it will be possible to verify whether the present approach can detect changes occurring in the musculoskeletal system.

With regard to the results, the values in Table II show that the average estimates of L_{oM}, F_{oM} and L_{TS} are consistent with physiological values as reported in [9, 16], with F_{oM} for extensors the only overestimated parameter. This might be explained by considering that the total torque exerted during extension experiments was ascribed to ECRL only. Among the three parameters, L_{TS} is seen to be the least sensitive and different optimization algorithms could be tested to improve the parameter identification process. Furthermore, it must be reported that the upper bound of L_{oM} for the flexors was frequently reached. Besides, once the estimated parameters were used as input to the model, the simulated torque closely follows the measured one (Fig. 3) with values of RMSE and NRMSE comparable to those found during the estimation phase at 0°. Moreover, the values regarding LOOCV present a similar outcome (Table II).

Fig. 4A shows a shallower trend with regard to the flexor moment variability when compared to data from [16-19]. In the works from [16-18] flexor moment peaks were mainly located in the flexed region, while in Garner and Pandy [9] the highest peak was located at 0°. In the present study the highest values were found in extended positions as also reported in [19] and in [22]. With regard to the extensors, Fig. 4B shows that torques were lower than flexor torques, as generally found in the literature. The measured highest peak was recorded at a

slightly flexed position (+10°), which contrasts with findings in [16-19] where peaks were mainly located in the extension region. However, measurements in Garner and Pandy [9] were similar to those of the present work with the highest peaks occurring in flexion. Nevertheless, it is worth noting the agreement between the measured and the predicted results.

As Fig. 5 shows, the trend of the force curves contrasts that of the *MAs*: as force increases (decreases), the *MA* decreases (increases). A comparison between Fig. 5A and Fig. 5B shows that estimated flexor forces are on average smaller than estimated extensor forces, even though flexor moments were higher than the extensor ones. This might be explained by looking at Fig. 6 and considering the values of the ratios L_{TS}/L_{oM} and L_{oM}/MA_{ave}. Fig. 6 shows that flexors are found to operate mainly on the ascending limb of the normalised force-length relationship with larger muscle length change than extensors which, instead, were characterized by a narrower range of motion at the top of the same curve. This behavior is consistent with values of the two ratio indexes. Indeed, a smaller value of L_{TS}/L_{oM} for extensors indicates stiffer musculotendon actuators with smaller muscle excursion predominantly located in the upper part of the ascending limb, hence higher forces, as also found in [8, 19]. At the same time, extensors are also characterized by a larger L_{oM}/MA_{ave} ratio [18-19]. As a consequence, a major role in the joint moment is played by the *MA*s more than muscle forces: even though extensors are characterized by larger forces than flexors, extensor torques are smaller because of the smaller values of *MA*. Fig. 6 also confirms findings in [18-19], even though in these works FCU was found to operate also at shorter lengths, while the range of motion of FCR in [18] was located on the plateau region of the force-length relationship. However, it must be emphasized that the results shown herein refer to FCU, FCR and FDS lumped together and the range of motion used during the experiments was smaller than the ones in the two cited works. With regard to the range of motion of

ECRL, its location at the top of the curve, which corresponds to slightly longer muscle lengths, confirms results in [18-19].

As a final comment, it has been shown [23] that, from a bottom-up perspective, the muscle mechanics plays an essential role in simplifying the problem of neuromuscular control as seen from the central nervous system, especially when lower limbs are concerned. In this framework, the present approach could be exploited to relate muscle mechanics and neuromuscular control or as a diagnostic tool to characterise the mechanics of targeted musculotendon units of the upper limbs for people affected by muscle disorders.

Conclusion

The present model has potential as an in vivo method to estimate musculotendon parameters. In particular, it was found that: the values of the estimated parameters varied in a range (Table II) consistent with physiological measurements; the model is able to simulate the measured torques with values of RMSE and NRMSE comparable to those calculated during the estimation phase (Table II and Fig. 3); the range of motion of the muscle fibers as well as the influence of tendon elasticity and *MAs* are consistent with findings in the literature (Table II and Fig. 6).

The simple one degree of freedom model has some limitations. Despite these, or if improved models were developed, the present approach could be used in conjunction with models of neurophysiologic pathways as a benchmark for characterizing biomechanical parameters of the musculotendon system with the aim of identifying deviations from normality in presence of neuromuscular pathologies.

Conflict of interest statement

None.

Acknowledgements

The authors would like to thank Dr. David Simpson for his help with the EMG linear envelope processing and Ruth Turk for her help with the test rig and the placement of the electrodes. Financial support provided by EPSRC (Platform Grant in Structural Acoustics) is also acknowledged.

Tables

TABLE 1 – MODEL PARAMETERS (SEE TEXT FOR DETAILS)

	Value
τ_{act}	0.05 [s]
τ_{deact}	0.08 [s]
d	0.56
k	$-1/d^2$
λ	0.15
aa	1.5
bb	8
cc	0.0866

TABLE 2 – ESTIMATED PARAMETERS

	Bounds	Estimated		Holzbaur et al. [16]	Garner and Pandy [9]
		Min/Max	Ave±σ		
Flexors					
L_{oM} **[cm]**	1/10	5.99/9.96	8.51 ± 1.14	6.65[a]	4.54[a]
F_{oM} **[N]**	20/2000	340/899	547± 126	429.5[b]	929.63[b]
L_{TS} **[cm]**	10/40	19.5/25.7	22.2 ± 0.03	22.4[a]	26.8[a]
A	-3/0	-2.11/0	-0.56 ± 0.52		
ΔL_{MT} **[cm]**	10% of values in [11]	-2.24/-1.17	-2.00 ± 0.72		
MA **[cm]**	10% of values in [11]	1.65/1.98	1.80 ± 0.15		
Extensors					
L_{oM} **[cm]**	1/Inf	7.74/11.9	9.14 ± 2.50	8.1	8.96
F_{oM} **[N]**	20/2000	341/1033	664 ± 179	304.9	268.42
L_{TS} **[cm]**	10/40	22.1/22.3	22.2 ± 0.03	22.4	26.8
A	-3/0	-0.51/0	-0.11 ± 0.11		
ΔL_{MT} **[cm]**	10% of values in [11]	-1.49/-1.38	-1.45 ± 0.42		
MA **[cm]**	10% of values in [11]	0.93/1.02	0.99 ± 0.15		

[a]Average of values in [9, 16] for FCU, FCR and FDS. [b]Sum of values in [9, 16] for FCU, FCR and FDS. Since the flexor electrodes were positioned equidistant from the FCU, FCR and FDS motor points, it was assumed that the recorded EMG represented the summative signal coming from these three muscles.

TABLE 3 – RMSE AND NRMSE VALUES

	Flexors			
	Estimation		Validation	
	Min/Max	Ave±σ	Ave±σ	Min-Max
RMSE [N]*	0.35/1.30	0.74 ± 0.17	0.90 ± 0.48	0.44-1.80
NRMSE [%]*	4.71/12.49	8.76 ± 1.66	10.36 ± 0.04	6.12-17.07
RMSE [N]**			0.94 ± 0.41	0.51-1.63
NRMSE [%]**			11.94 ± 9.21	7.26-23.15
	Extensors			
RMSE [N]*	0.16/0.56	0.39 ± 0.08	0.49 ± 0.15	0.23-0.70
NRMSE [%]*	4.68/8.24	6.51 ± 1.01	7.80 ± 1.83	5.40-11.32
RMSE [N]**			0.58 ± 0.32	0.27-0.85
NRMSE [%]**			9.97 ± 5.51	8.03-14.45

*Validation carried out at 0°. **Leave-one-out cross-validation.

TABLE 4 – MOMENTS, ESTIMATED FORCES AND INDEXES (L_{TS}/L_{OM} AND L_{OM}/MA_{AVE})

	Flexors			Extensors		
	Min	**Max**		**Min**	**Max**	
$\mathbf{M_{meas}}^{\dagger}$ **[Nm]**	6.25	15.95		2.71	10.96	
$\mathbf{M_{pred}}^{\dagger}$ **[Nm]**	5.72	14.73		3.61	11.51	
$\mathbf{M^{TOT}_{meas}}^{\dagger\dagger}$ **[Nm]**	9.13 ± 1.14			6.38 ± 1.10		
$\mathbf{M^{TOT}_{pred}}^{\ddagger\ddagger}$ **[Nm]**	8.67 ± 0.73			6.43 ± 1.08		
$\mathbf{F_{EST\ I}}$ **[N]**	454.54			697.49		
$\mathbf{F_{EST\ II}}$ **[N]**	558.75			682.83		
	Min	**Ave±σ**	**Max**	**Min**	**Ave±σ**	**Max**
L_{TS}/L_{oM}	2.55	2.94 ± 0.53	4.06	1.87	2.47± 0.32	2.87
$L_{oM}/MA_{ave}{}^{\#}$	3.37	4.69 ± 0.79	5.87	7.66	9.18± 1.23	11.66

†Occurred between -30° and +30°. ††Average over nine subjects. ‡‡Average over ten subjects. $^{\#}MA_{ave}$ was calculated by averaging the moment arms for each subject across the range of motion.

Figure Captions

Figure Captions

Fig. 1. Schematic representation of the neuromusculoskeletal model. Recorded EMGs determine the muscle activation level, which contributes to generate muscle and tendon force as well as joint moments once coupled with a model of the limb anatomy.

Fig. 2. Test. For flexors, the EMG electrodes were placed on a line from the medial epicondyle of the elbow to the radial styloid process (base of the thumb), one third distal of the medial epicondyle. For extensors, they were placed on a line from the lateral epicondyle of the elbow to the 2nd metacarpal, 5-7cm distal of the lateral epicondyle.

Fig. 3. Validation at 0° for Subject 12. A) Flexors; B) Extensors. Torques: calculated (dot-dash) and measured (thick). Linear Envelope EMGs: agonists (dot) and antagonists (dash). EMGs of flexors and extensors were used as input to the model in A and B, respectively. The EMGs of the antagonists are plotted for convenience only and were not involved at this stage of the work. EMG values are normalised as specified in the text and vary between 0 and 1.

Fig. 4. Torques vs. wrist joint angles: A) Flexors; B) Extensors. Solid lines represent average (±SD) maximum isometric measured and calculated moments in the present study. Each point is the average over nine and ten subjects for flexors and extensors, respectively. The largest moments occurred at -30° (A) and +10° (B). The wrist as modelled in the work from Gonzalez et al. [18] reproduced recorded data as reported in [17], while the wrist as modelled in [9] was compared to measurements carried out during the same study. Measured values

from [17] were averaged over ten subjects. Measured values from [9] were averaged over three subjects. Flexion angles are positive, extension angles are negative.

Fig. 5. Average maximum calculated force and *MA*s vs. wrist joint angle: A) Flexors; B) Extensors. Averages calculated over nine and ten subjects, respectively. The highest forces occurred at -30° (A) and +30° (B). Flexion angles are positive, extension angles are negative.

Fig. 6. Continuous line: normalised force-length relationship of muscles. Diamond markers: average operating range of wrist flexors. Triangle markers: average operating range of wrist extensors. Dotted lines: operating range of FCU and ECRL in [18]. Dashed lines: operating range of FCU and ECRL in [19].

Figures

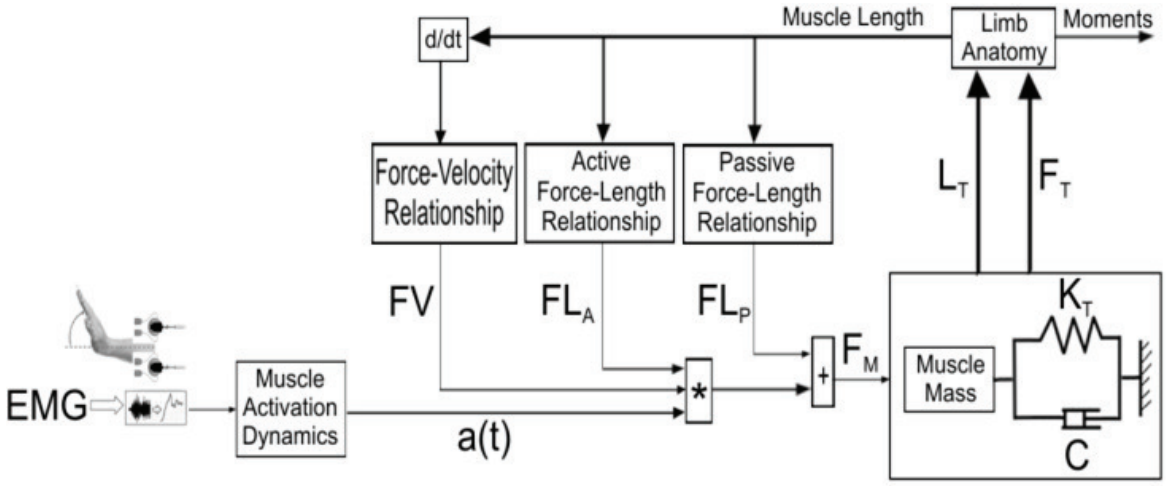

Figure 1

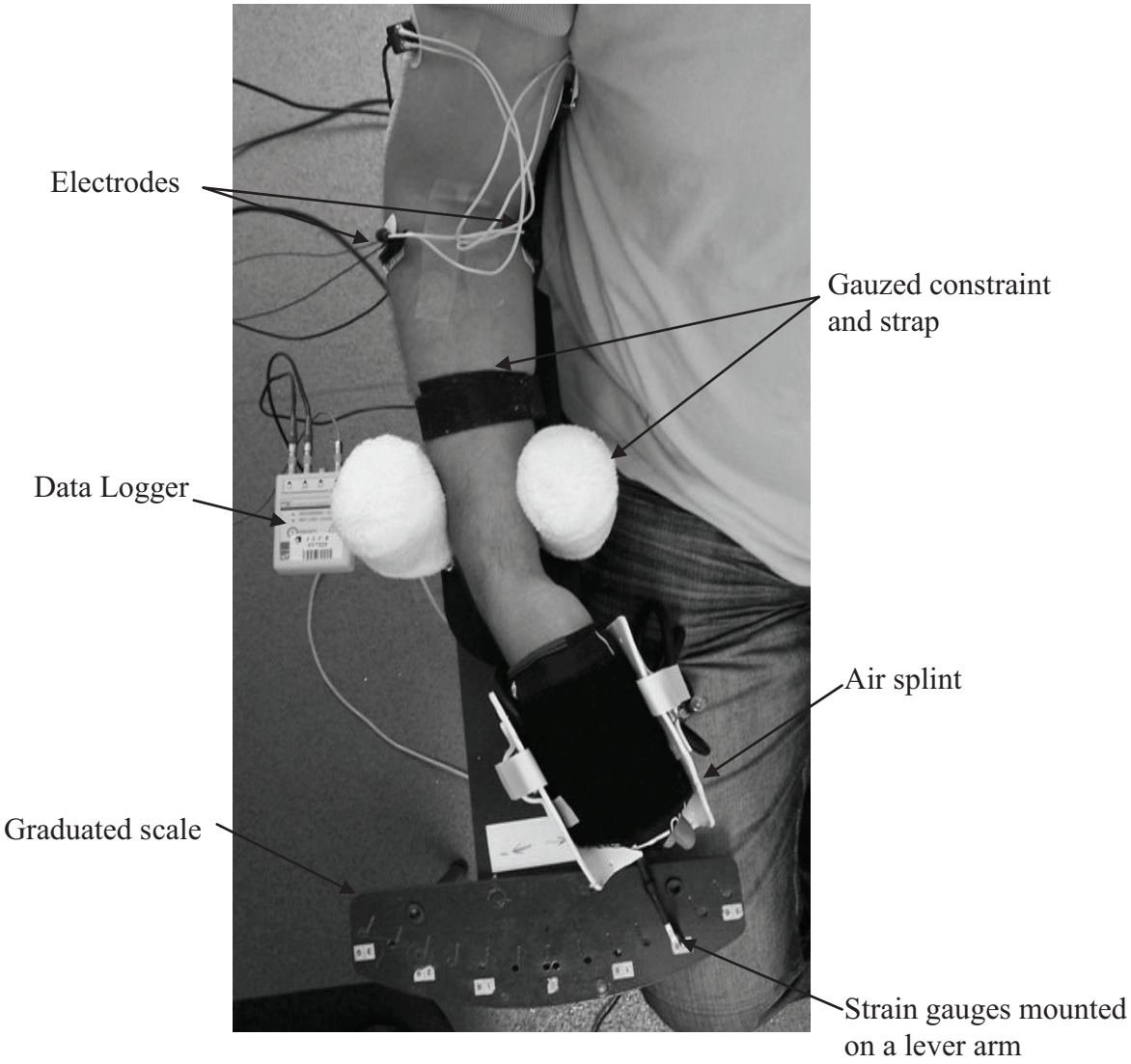
Electrodes
Gauzed constraint and strap
Data Logger
Air splint
Graduated scale
Strain gauges mounted on a lever arm

Figure 2

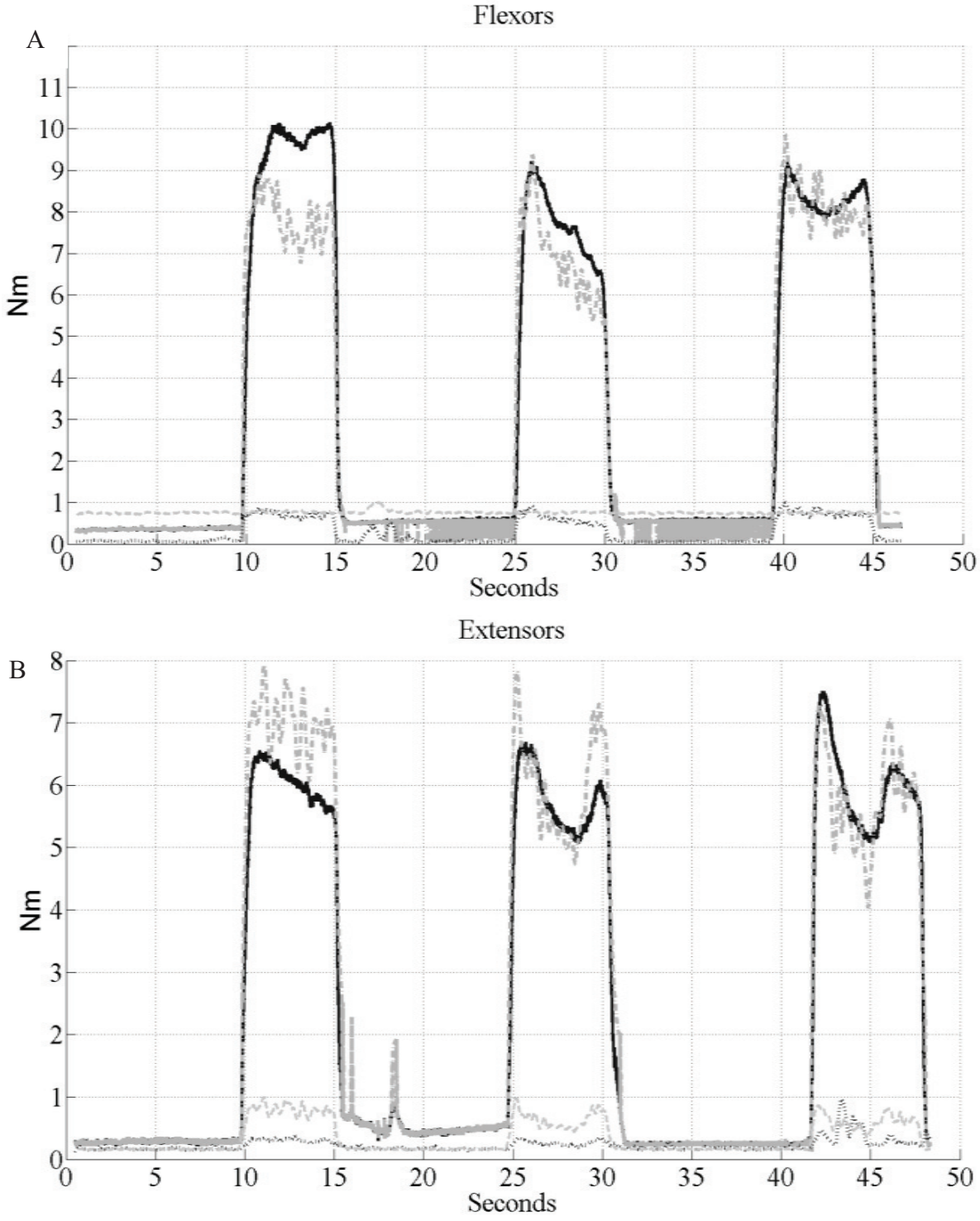

Figure 3

A

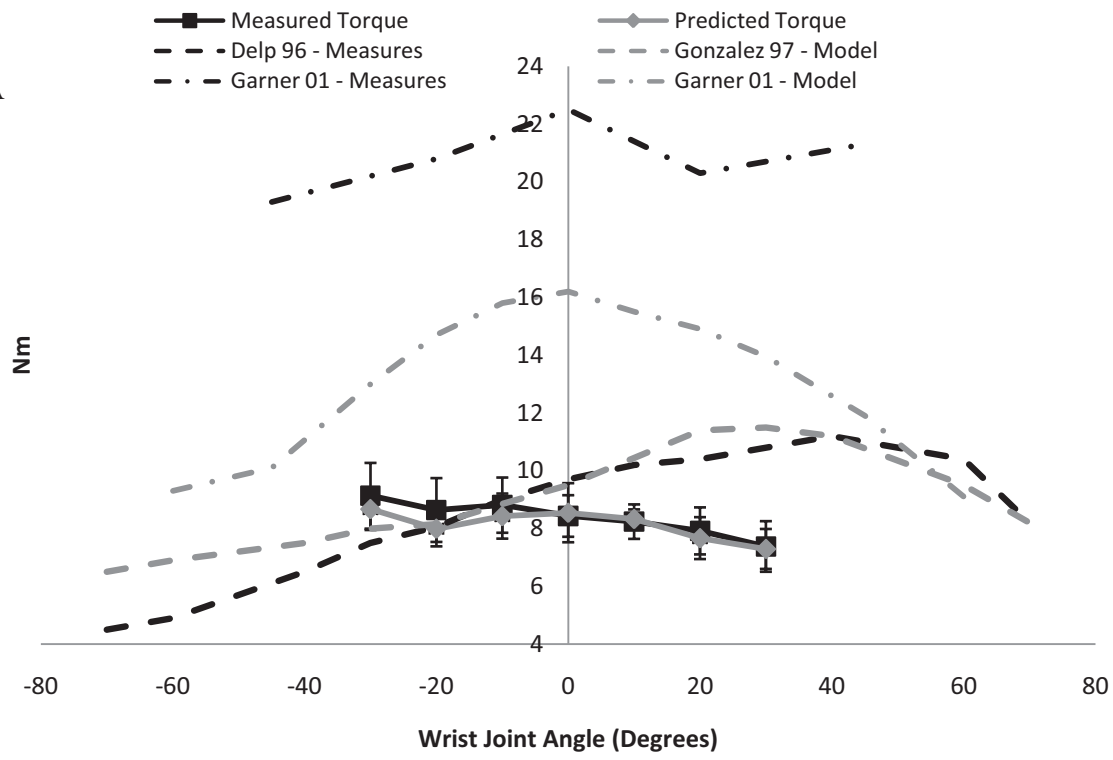
Measured Torque
Predicted Torque
Delp 96 - Measures
Gonzalez 97 - Model
Garner 01 - Measures
Garner 01 - Model
Nm
24
22
20
18
16
14
12
10
8
6
4
-80
-60
-40
-20
0
20
40
60
80
Wrist Joint Angle (Degrees)

B

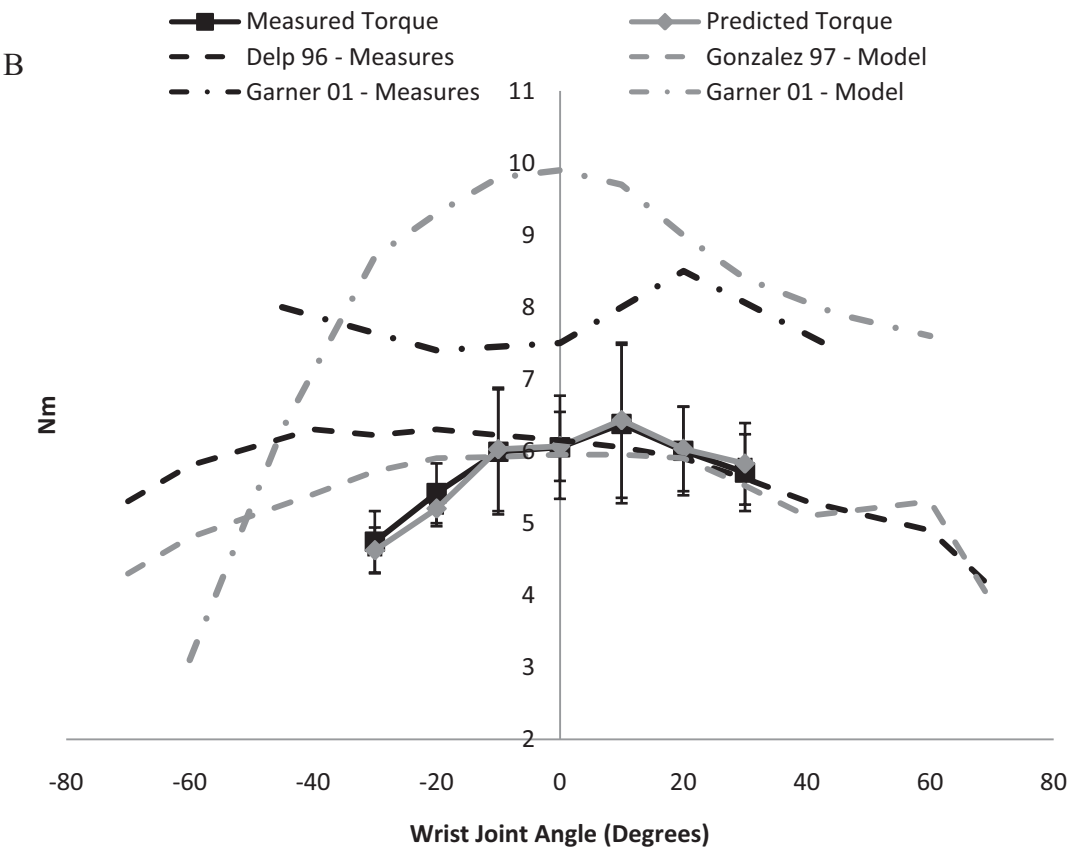
Measured Torque
Predicted Torque
Delp 96 - Measures
Gonzalez 97 - Model
Garner 01 - Measures
Garner 01 - Model
Nm
11
10
9
8
7
6
5
4
3
2
-80
-60
-40
-20
0
20
40
60
80
Wrist Joint Angle (Degrees)

Figure 4

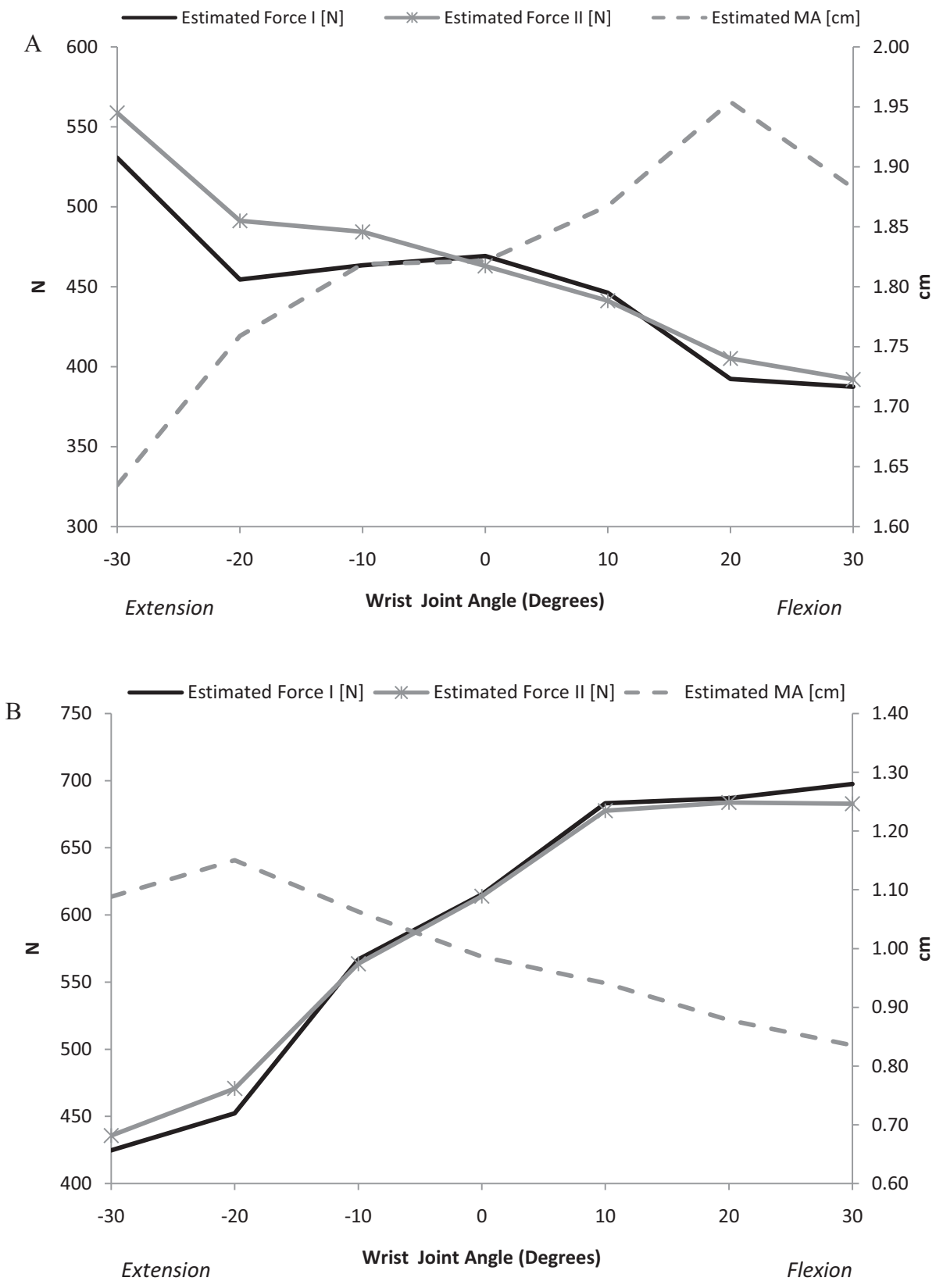
A
Estimated Force I [N]
Estimated Force II [N]
Estimated MA [cm]
N
cm
600
550
500
450
400
350
300
2.00
1.95
1.90
1.85
1.80
1.75
1.70
1.65
1.60
-30
-20
-10
0
10
20
30
Extension
Wrist Joint Angle (Degrees)
Flexion
B
Estimated Force I [N]
Estimated Force II [N]
Estimated MA [cm]
N
cm
750
700
650
600
550
500
450
400
1.40
1.30
1.20
1.10
1.00
0.90
0.80
0.70
0.60
-30
-20
-10
0
10
20
30
Extension
Wrist Joint Angle (Degrees)
Flexion

Figure 5

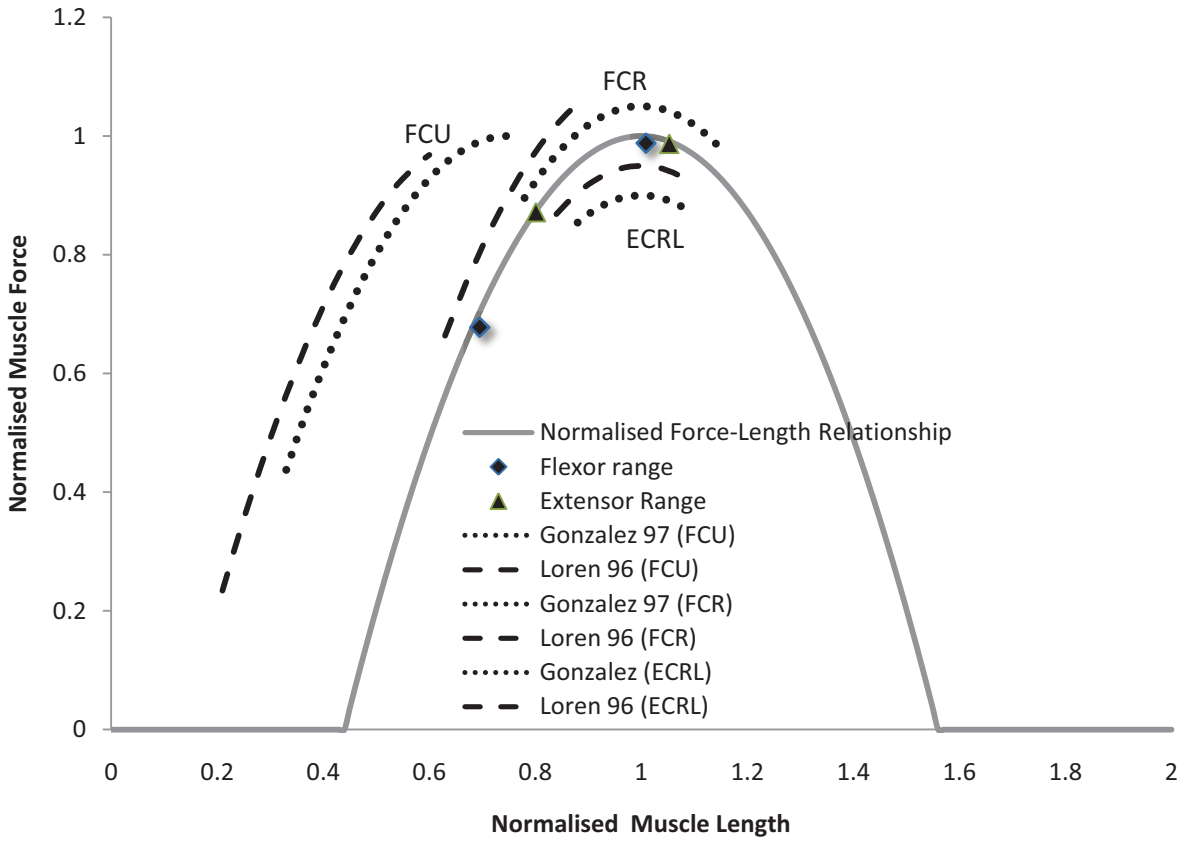
1.2
1
0.8
0.6
0.4
0.2
0
Normalised Muscle Force
0
0.2
0.4
0.6
0.8
1
1.2
1.4
1.6
1.8
2
Normalised Muscle Length
FCR
FCU
ECRL
Normalised Force-Length Relationship
Flexor range
Extensor Range
Gonzalez 97 (FCU)
Loren 96 (FCU)
Gonzalez 97 (FCR)
Loren 96 (FCR)
Gonzalez (ECRL)
Loren 96 (ECRL)

Figure 6

References.

[1] Peckham PH, Knutson JS. Functional electrical stimulation for neuromuscular applications. Annual review of biomedical engineering. 2005;7:327-60.
[2] Langhorne P, Coupar F, Pollock A. Motor recovery after stroke: a systematic review. Lancet neurology. 2009;8:741-54.
[3] Pearson K, Ekeberg O, Buschges A. Assessing sensory function in locomotor systems using neuro-mechanical simulations. Trends in neurosciences. 2006;29:625-31.
[4] Lloyd D, Besier T, Winby C, Buchanan TS. Neuromusculoskeletal modelling and simulation of tissue loading in lower extremities. In: Hong Y, Bartlett R, editors. Routledge Handbook of Biomechanics and Human Movement Science London and New York: Taylor & Francis Group; 2009.
[5] Buchanan TS, Lloyd DG, Manal K, Besier TF. Neuromusculoskeletal modeling: estimation of muscle forces and joint moments and movements from measurements of neural command. Journal of applied biomechanics. 2004;20:367-95.
[6] Erdemir A, McLean S, Herzog W, van den Bogert AJ. Model-based estimation of muscle forces exerted during movements. Clinical biomechanics (Bristol, Avon). 2007;22:131-54.
[7] Koo TK, Mak AF, Hung LK. In vivo determination of subject-specific musculotendon parameters: applications to the prime elbow flexors in normal and hemiparetic subjects. Clinical biomechanics (Bristol, Avon). 2002;17:390-9.
[8] Zajac FE. Muscle and tendon: properties, models, scaling, and application to biomechanics and motor control. Crit Rev Biomed Eng. 1989;17:359-411.
[9] Garner BA, Pandy MG. Musculoskeletal model of the upper limb based on the visible human male dataset. Comput Methods Biomech Biomed Engin. 2001;4:93-126.
[10] Lan N. Stability analysis for postural control in a two-joint limb system. IEEE Trans Neural Syst Rehabil Eng. 2002;10:249-59.
[11] Lemay MA, Crago PE. A dynamic model for simulating movements of the elbow, forearm, an wrist. J Biomech. 1996;29:1319-30.
[12] Mendez J, Keys A. Density and composition of mammalian muscle. Metabolism, Clinical and Experimental. 1960;9:184-8.
[13] Holzbaur KR, Murray WM, Gold GE, Delp SL. Upper limb muscle volumes in adult subjects. Journal of biomechanics. 2007;40:742-9.
[14] Winter D. Biomechanics and motor control of human movement. 3rd ed: Wiley; 2005.
[15] Khoo MCK. Physiological Control Systems: Analysis, Simulation, and Estimation. New York: Wiley, John & Sons, Inc.; 1999.
[16] Holzbaur KR, Murray WM, Delp SL. A model of the upper extremity for simulating musculoskeletal surgery and analyzing neuromuscular control. Ann Biomed Eng. 2005;33:829-40.
[17] Delp SL, Grierson AE, Buchanan TS. Maximum isometric moments generated by the wrist muscles in flexion-extension and radial-ulnar deviation. J Biomech. 1996;29:1371-5.
[18] Gonzalez RV, Buchanan TS, Delp SL. How muscle architecture and moment arms affect wrist flexion-extension moments. J Biomech. 1997;30:705-12.
[19] Loren GJ, Shoemaker SD, Burkholder TJ, Jacobson MD, Friden J, Lieber RL. Human wrist motors: biomechanical design and application to tendon transfers. J Biomech. 1996;29:331-42.
[20] Lieber RL. Skeletal muscle structure and function - implicationsfor rehabilitation and sports medicine. Baltimore: Williams & Wilkings; 1992.
[21] Blemker SS, Asakawa DS, Gold GE, Delp SL. Image-based musculoskeletal modeling: applications, advances, and future opportunities. J Magn Reson Imaging. 2007;25:441-51.

[22] Hutchins EL. The musculoskeletal geometry of the human elbow and wrist: An analysis using torque-angle relationships. Austin: University of Texas at Austin; 1993.
[23] Hof AL. Muscle mechanics and neuromuscular control. Journal of biomechanics. 2003;36:1031-8.

***Referee Suggestions**

Emer P. Doheny

e-mail: doheny@ucd.ie

School of Electrical, Electronic and Mechanical Engineering

University College Dublin

Ireland

Wei Tech Ang

e-mail: wtang@ntu.edu.sg

School of Mechanical & Aerospace Engineering

Nanyang Technological University

Singapore.

Tobias Siebert

e-mail: tobias.siebert@uni-jena.de

Institute of Motion Science

Friedrich Schiller University

Seidelstraße 20, 07749 Jena

Germany